JOURNAL OF APPLIED ELECTROCHEMISTRY **16** (1986) 719–731

The electrochemical behaviour of silver sulphide in sulphuric acid solutions

D. W. PRICE, G. W. WARREN, B. DROUVEN*

Department of Metallurgical Engineering and Materials Science, Carnegie-Mellon University, Schenley Park, Pittsburgh, PA 15213, USA

Received 12 July 1985; revised 25 November 1985

The electrochemical behaviour of synthetic silver sulphide (acanthite) electrodes in sulphuric acid solutions has been investigated using several techniques including cyclic voltammetry, anodic polarization and constant potential experiments. Under anodic polarization the dissolution has been attributed to the reaction $Ag_2S = 2Ag^+ + S + 2e$ which occurs in two sequential, single electron transfer steps. A kinetic model for this stepwise anodic dissolution process at lower overpotential, where the current is a function of potential, is provided. At high dissolution rates (i.e. high currents) the slightly soluble silver sulphate salt is formed on the surface due to the saturation of the electrolyte near the Ag_2S interface. This observation is supported by the influence of electrolyte composition on the cyclic voltammetry and the polarization curve. A paralinear film growth model has been found to describe the formation and growth of the silver sulphate product layer indicating an initial region of parabolic kinetics which gradually changes to linear kinetics as the rate of film dissolution approaches that of film formation.

1. Introduction

Small additions of silver ion have a catalytic effect on the leaching of copper from chalcopyrite in ferric sulphate solutions. Researchers have reported that as little as 72 p.p.m. of an initially soluble silver compound significantly enhances the extent and rate of leaching [1]. Pawlek [2] has found that for oxygen leaching of attrition-ground chalcopyrite, 30 min was required to extract 51% of the copper at 100° C. With the addition of silver catalyst under identical conditions, 95% of the copper was extracted in the same length of time. The dissolved silver was added in very small amounts, i.e. only 0.75% of the weight of the chalcopyrite. Investigations of the mechanism of this apparent catalysis have not been reported except in some work by Miller and Portillo [3], who have shown that the silver ion reacts with the chalcopyrite, forming a Ag_2S layer on the mineral surface. Although the exact mechanism of the catalysis is not known, the involvement of this Ag_2S film has been proposed in the following mechanism [3]:

$$4Ag^+ + CuFeS_2 = 2Ag_2S + Cu^{2+} + Fe^{2+}$$

$$2Fe^{3+} + Ag_2S = 2Ag^+ + S + 2Fe^{2+}$$

While the first reaction has been verified experimentally, the occurrence of the second reaction has not yet been proven. Therefore, a study of the feasibility of the above catalytic mechanism would benefit by an examination of the anodic behaviour of Ag_2S in sulphuric acid solutions. Previous work has concerned the development of the $Ag–S–H_2O$ Pourbaix diagram and its verification, primarily with galvanostatic and potentiostatic techniques [4]. The present study begins with an examination of cyclic voltammetry of Ag_2S in H_2SO_4 solutions. Combined with previously reported

* *Present address:* Preussag AG, Goslar, West Germany.

0021–891X/86 $03.00 + .12 © 1986 Chapman and Hall Ltd.

galvanostatic and potentiostatic experiments, the cyclic voltammetry provides a more complete picture of the electrochemistry of the Ag_2S. With this more thorough electrochemical description, the initial anodic dissolution of silver sulphide is examined more closely through kinetic models. The models are used to analyse the dissolution process at lower overpotentials where the current (i.e. rate) is a function of potential and at high overpotentials were current is independent of potential.

2. Experimental procedure

The Ag_2S used was produced by bubbling H_2S through an aqueous $AgNO_3$ solution. The precipitated Ag_2S was collected by filtration, washed and dried. X-ray diffraction and energy dispersive X-ray analysis were used to verify the composition of the silver sulphide and showed no other material present. The material was used to produce two types of electrode, cast and pressed pellets. The cast samples were prepared by melting Ag_2S in a cylindrical mold under a sulphur atmosphere, thereby suppressing decomposition. Slow cooling ensured the transition from argentite to acanthite. The pellet samples were produced by pressing a mixture of 80% Ag_2S and 20% graphite (Monarch 800, Cabot Corporation) into a 1.20-cm diameter pellet. In this way the graphite lowered the resistance through the Ag_2S electrode, and the measurement of the *IR* drop through the pellet was minimized. With hydraulic pressing, the pellets attained 97% theoretical density, having corrected for graphite content. In order to avoid potential problems with porosity the samples were impregnated with a low viscosity resin (Spurr Epoxy). The use of two types of electrode was found to be necessary for several reasons. Cast samples were needed in order to represent more closely a surface which consisted entirely of Ag_2S. Pellet electrodes containing carbon were used primarily for cyclic voltammetry as the current peaks were generally more easily detected and more well defined than for the cast samples, although the shape of the voltammetric response was the same for both types.

Copper wire was attached to both cast and pellet samples with a silver-based conductive cement (Epo-Tek E, Epoxy Technologies). The wire was covered with glass tubing and the assembly was embedded in epoxy resin. For rotating disc studies, electrodes were produced from Ag_2S pellets, attached with silver cement to a Teflon-surrounded stainless steel tip. The tip could then be screwed onto the rotating assembly. All electrodes were wet ground through 600 grit carborundum paper and washed with distilled water before insertion into the electrochemical cell. All solutions were prepared with reagent grade chemicals and distilled, deionized water.

Experiments were performed in a 1-litre vessel with a Luggin capillary separating the reference electrode compartment from the bulk electrolyte. A sintered glass frit separated the compartment containing the platinum counter electrode from the bulk electrolyte. A saturated calomel reference electrode was used for all experiments, but all values of potential given in this paper have been converted to standard hydrogen electrode (SHE). The electrochemical equipment was comprised of a Princeton Applied Research (PAR) 173 potentiostat with 376 log current converter, a PAR 175 voltage programmer and an X–Y recorder. Rotating disc experiments were performed with a Pine instruments analytical rotator with ASR speed control assembly. All rotation speeds were verified with a digital stroboscope.

3. Results and discussion

3.1. *Analysis of cyclic voltammetry*

Cyclic voltammetry was conducted for both cast and pressed Ag_2S in various sulphuric acid solutions as shown in Figs 1–3. The initial direction of the potential sweep is anodic for all the data shown in Figs 1–3. Combining the voltammetry with reactions predicted from the Ag–S–H_2O Pourbaix diagram and earlier experiments [4] results in a more complete understanding of the

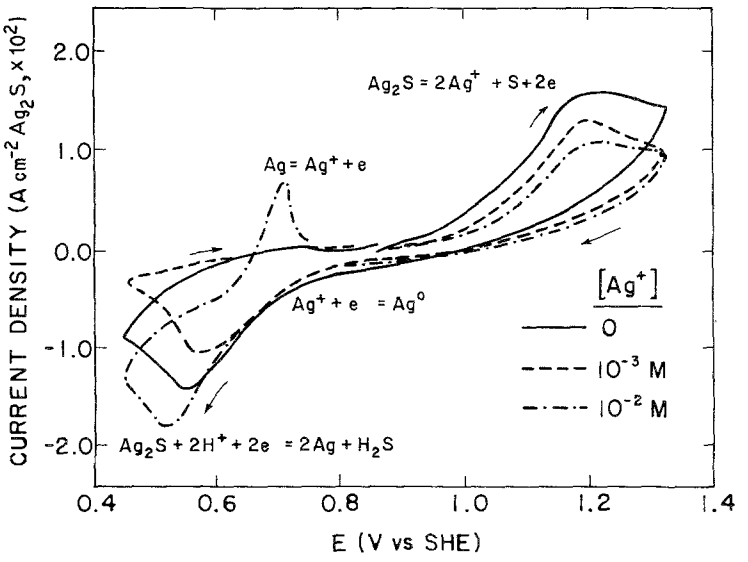

Fig. 1. Cyclic voltammograms for pressed pellets of Ag_2S in 1.0 M H_2SO_4 solutions with varying additions of silver ion. Sweep rate, 0.01 V s^{-1}.

electrochemistry of Ag_2S. The cast and pressed samples were quite similar in behaviour, the only difference being an increase of 0.20 V in the rest potential for the pressed samples, presumably due to the presence of the added graphite.

Fig. 1 shows the voltammograms for pressed Ag_2S pellets in 1 M H_2SO_4 with various concentrations of Ag^+, added in the form of $AgNO_3$. Rest potentials increase approximately 0.06 V with a one decade increase in Ag^+ concentration, in agreement with previous data [4], which proposed the following potential determining reaction:

$$Ag_2S = 2Ag^+ + S + 2e \quad (1)$$

$$E = 1.008 + 0.059 \log[Ag^+]$$

As the electrode potential is increased from the rest potential, a rise in current occurs, continuing up to about 1.2 V. While the Pourbaix diagram indicates a number of possible reactions for creating this current, those which produce metallic silver as a product are not considered since no metallic silver could be found on the electrode during anodic cycling or in constant potential experiments

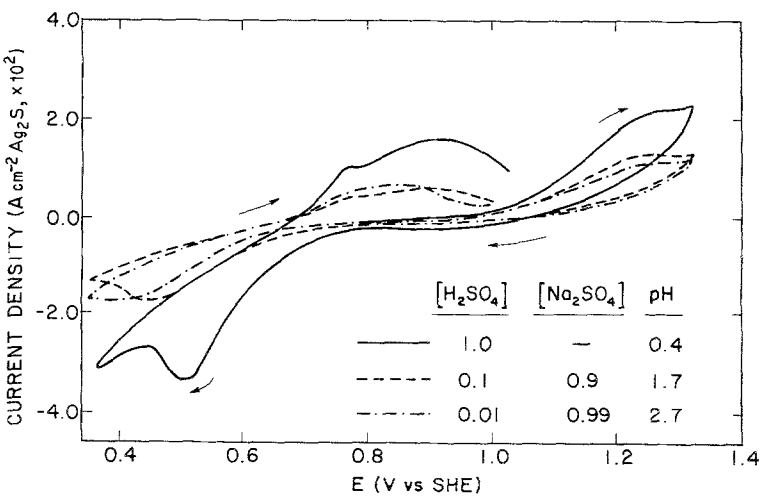

Fig. 2. Cyclic voltammograms for pressed pellets of Ag_2S in solutions with varying pH and constant ionic strength. Sweep rate, 0.01 V s^{-1}.

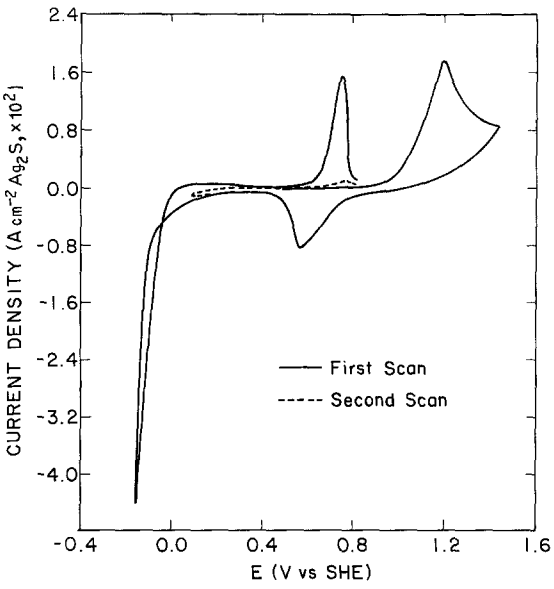

Fig. 3. Cyclic voltammogram for a pressed pellet of Ag_2S in 1.0 M H_2SO_4 showing the effect of a change in the cathodic limit. Sweep rate, 0.01 V s^{-1}.

carried out for extended times [4]. Dissolved Ag^+, on the other hand, was detected in the electrolyte by atomic absorption. Therefore, the initial current rise could result from any of the following reactions.

$$Ag_2S = 2Ag^+ + S + 2e \quad (1)$$

$$E = 1.008 + 0.059 \log[Ag^+]$$

$$Ag_2S + 4H_2O = 2Ag^+ + HSO_4^- + 7H^+ + 8e \quad (2)$$

$$E = 0.506 + 0.007 \log[Ag^+]^2[HSO_4^-] - 0.052\,pH$$

$$Ag_2S + 4H_2O = 2Ag^+ + SO_4^{2-} + 8H^+ + 8e \quad (3)$$

$$E = 0.520 + 0.007 \log[Ag^+]^2[SO_4^{2-}] - 0.059\,pH$$

Reactions similar to reaction 1 have been reported for PbS, ZnS and FeS_2 [5–8]. Current efficiency calculations from potentiostatic and galvanostatic experimentation have been reported and indicate that the initial oxidation occurs by way of reaction 1, while reactions 2 and 3 play a more important role at higher potentials [4].

Based on results obtained in this and a previous study, the decrease in current observed at potentials higher than about 1.20 V on Fig. 1 is attributed to a covering of the electrode surface with Ag_2SO_4[4]. This sulphate formation would occur when the boundary layer of the electrode becomes saturated with Ag^+ and SO_4^{2-}. This was confirmed in that silver sulphate was detected on the electrode surface by scanning electron microscopy (SEM) and X-ray diffraction following an anodic galvanostatic treatment in 1 M H_2SO_4 where the bulk silver ion concentration was less than saturation. Other investigators have reported that a similar passivation phenomenon, which occurs during the dissolution of PbS in HCl solutions, is caused by the formation of $PbSO_4$ and sulphur, along with $PbCl_2$ [9].

The cyclic voltammograms in Figs 1 and 2 provide further information on Ag_2SO_4 deposition. If the current peak at 1.2 V is indeed caused by a covering of the electrode surface with Ag_2SO_4, electrolytes with higher Ag^+ concentrations should exhibit a lower amount of charge passed upon reaching the peak potential. At lower bulk Ag^+ concentrations, additional Ag^+ would be required to saturate the boundary layer involving additional charge transfer from reactions 1–3. Using the

Table 1. Calculation of the charge passed and expected [Ag^+] concentration in the initial anodic sweep for the data given in Fig. 1

Electrolyte	*Charge passed to peak (C)*	*Calculated concentration of Ag^+ in boundary layer (M)*
1 M H_2SO_4	0.813	7.45
1 M H_2SO_4/10^{-3} M Ag^+	0.203	1.85
1 M H_2SO_4/10^{-2} M Ag^+	0.158	1.43

current and potential sweep rates provided in Fig. 1, the charge passed from the start of the anodic scan to the peak can be calculated. Results are given in Table 1 and, as expected, less charge is passed for electrolytes with higher Ag^+ concentration. By assuming that no Ag^+ leaves the boundary layer and assuming a minimum boundary layer thickness of 1×10^{-3} cm, the Ag^+ concentration near the electrode surface may be estimated, neglecting the formation of Ag_2SO_4. These values are also given in Table 1. The solubility limit for the formation of Ag_2SO_4 in 1 M H_2SO_4 solutions is 0.071 M Ag^+ at 25° C [10]. For all solutions listed in Table 1, this value is exceeded. Even if the assumption that no Ag^+ leaves the boundary layer is relaxed, the formation of Ag_2SO_4 is still indicated, since removal of roughly 95% of the Ag^+ produced would be required to prevent the precipitation of Ag_2SO_4. This extent of Ag^+ diffusion is not feasible during the short time of the scan.

The effect of pH on the initial anodic scan is shown in Fig. 2 The sulphate concentration, and hence ionic strength, was kept relatively constant by means of Na_2SO_4 additions. In many scans the initial anodic region showed no strong pH dependency, but in several trials the anodic current increased slightly with decreasing pH, as seen in Fig. 2. Lietzke and Stoughton [11] determined solubility values for Ag_2SO_4 as a function of hydrogen ion concentration in various H_2SO_4 solutions and reported a slight increase in the solubility of Ag_2SO_4 as pH decreases. Therefore, lower pH solutions would require additional Ag^+ for saturation of the boundary layer. With less Ag_2SO_4 deposition, slightly higher current levels would be expected at lower pH (Fig. 2).

When the direction of the potential scan is reversed at approximately 1.3 V, the current and the dissolution of Ag_2S due to reaction 1 decrease, the Ag^+ concentration in the boundary layer also decreases and Ag_2SO_4 begins to dissolve. At about 0.95 V the current changes from anodic to cathodic and steadily increases up to the first cathodic peak at about 0.5 to 0.55 V (Figs 1, 2). There are several possible reductions to which this peak may be attributed; for consistency these are written as oxidations with the corresponding Nernst equations as follows.

$$Ag = Ag^+ + e \tag{4}$$

$$E = 0.799 + 0.059 \log[Ag^+]$$

$$2Ag + H_2S = Ag_2S + 2H^+ + 2e \tag{5}$$

$$E = -0.067 - 0.059\,pH - 0.0295 \log[H_2S]$$

$$H_2S = S + 2H^+ + 2e \tag{6}$$

$$E = 0.142 - 0.059\,pH - 0.0295 \log[H_2S]$$

The direct reduction of Ag_2SO_4 is highly unlikely since it is a poor conductor and is not in intimate contact with the Ag_2S surface due to the elemental sulphur which is also produced.

Based on the data of Figs 1–3 the peak at 0.50–0.55 V is attributed to the reduction of Ag^+ (reaction 4). Silver ion is present in the boundary layer from the previous anodic scan or from the dissolution of precipitated Ag_2SO_4. Thermodynamics would predict such a reduction at 0.68 V for 10^{-2} M [Ag^+], and as shown in Figs 1 and 2 the current does begin to increase substantially at this point. The position of the peak may be somewhat shifted to lower potentials due to slow dissolution

of Ag_2SO_4 or perhaps due to an overpotential associated with Ag^+ deposition on Ag_2S. An addition of Ag^+ should thus promote larger currents in this region, and this effect is indeed visible in Fig 1. In all trials the electrolyte with 10^{-2} M Ag^+ produced the highest current densities. However, comparing solutions with lower Ag^+ concentrations, a clear trend in peak current densities was not always observed; this is probably due to slight differences in morphology of the Ag_2SO_4 and elemental sulphur products formed from run to run and the resulting effect on the area of Ag_2S exposed.

Continuing the scan to more negative potentials prior to reversal, a second cathodic current peak is observed at approximately -0.12 V which is a result of the direct reduction of the Ag_2S to metallic silver via reaction 5, as shown in the first cycle of Fig. 3. Elemental silver can be observed and the odour of H_2S detected by holding the electrode at this potential for a few minutes. The direct reduction of Ag_2S has also been reported in previous investigations in acid [4] as well as alkaline electrolytes [12, 13]. Upon reversal of the scan, the current switches quickly to anodic, which presumably represents the oxidation of H_2S to sulphur (reaction 6). With slower stirring rates the H_2S produced by reaction 6 remains for a longer time near the electrode surface, resulting in predictably higher current values for the oxidation of H_2S.

With further oxidation a second and larger peak occurs at approximately 0.70 V as shown in Figs 1 and 3. It is in this region that the oxidation of metallic silver to Ag^+ (reaction 4) is thermodynamically predicted. This peak is very dependent on Ag^+ concentration, increasing greatly as Ag^+ concentration increases. Fig. 1 shows this trend clearly with a most distinct peak occurring in 10^{-2} M Ag^+. In electrolytes with added Ag^+, more silver is plated during the cathodic scan and, therefore, more silver is subsequently oxidized in the anodic portion of the scan. Cyclic voltammetry also shows no dependence on the sulphate concentration in this region, as expected from reaction 4. This peak is particularly evident in the first cycle of Fig. 3. Having already scanned to a cathodic limit of -0.20 V, silver was produced by the reduction of not only Ag^+ but also Ag_2S, and subsequently the peak associated with silver oxidation is large. On the next scan, partially shown in Fig. 3, the cathodic limit is raised to prevent the direct reduction of Ag_2S and silver is produced only by reaction 4 during the shortened cathodic treatment. Hence, a much smaller peak attributed to silver oxidation, at approximately 0.70 V, is expected and demonstrated on the second cycle.

3.2. *Modelling of the anodic polarization curve at low overpotentials*

In addition to the cyclic voltammetry just discussed, potentiodynamic polarization curves have also been performed in H_2SO_4 containing various additions of dissolved silver as shown in Fig. 4. A cast sample of Ag_2S was used in this case in order to simulate more closely a pure Ag_2S surface without the presence of carbon. In the previous section, evidence was presented to attribute the initial anodic dissolution of silver sulphide to reaction 1. Also at higher potentials the electrolyte near the surface becomes saturated and Ag_2SO_4 precipitates, at which point the dissolution rate becomes limited by the solubility of Ag_2SO_4. It seems reasonable to assume that, at least initially, the dissolution would be described by a charge transfer-limited process. However, when two or more electrons appear in an overall electrode reaction it is possible that the reaction actually occurs in two sequential, single electron charge transfer reactions. In other words it is possible that this dissolution occurs in a stepwise fashion, with reaction 1 being the overall result of the sequential reactions. In fact there seems to be some evidence that the simultaneous transfer of two electrons is energetically unfavourable [14, 15]. In order to evaluate this type of mechanism, a mathematical model for the stepwise dissolution process has been developed from electrode kinetic theory.

Two possible mechanisms for the dissolution in a two-step process are

$$Ag_2S = Ag^+ + AgS + e \tag{7}$$

$$AgS = Ag^+ + S + e \tag{8}$$

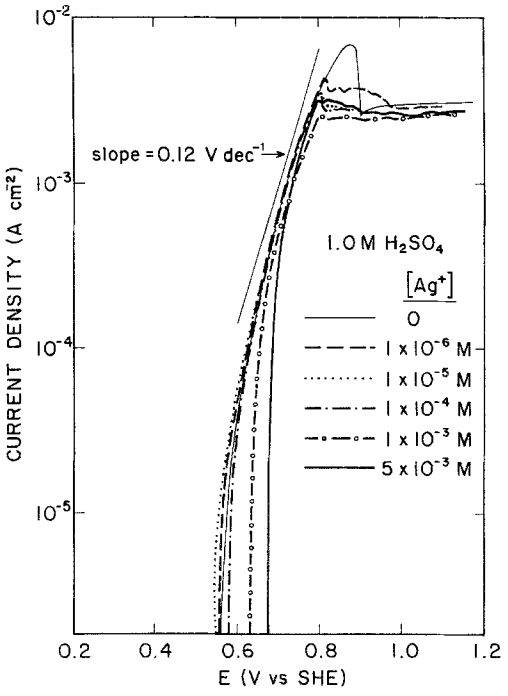

Fig. 4. Anodic polarization curves for a cast sample of Ag_2S in 1.0 M H_2SO_4 as a function of silver ion concentration Sweep rate, 0.001 V s^{-1}.

and

$$Ag_2S = 2Ag^+ + S^- + e \tag{9}$$

$$S^- = S + e \tag{10}$$

The mathematical kinetic treatment is the same for both cases. AgS and S^- are both short-lived intermediate species. A similar intermediate species has been proposed for the cathodic reduction of PbS electrodes [16]. A Butler–Volmer equation can be written for each individual step in the mechanism, and each step would carry one half of the total current, i_a.

$$0.5i_a = i_{0,1}\left\{\exp\left[\frac{\beta_1 F}{RT}\eta\right] - \frac{c_i}{\bar{c}_i}\exp\left[-\frac{(1-\beta_1)F}{RT}\eta\right]\right\} \tag{11}$$

$$0.5i_a = i_{0,2}\left\{\frac{c_i}{\bar{c}_i}\exp\left[\frac{\beta_2 F}{RT}\eta\right] - \exp\left[\frac{(1-\beta_2)F}{RT}\eta\right]\right\} \tag{12}$$

where $i_{0,1}$ is the exchange current density for step 1; $i_{0,2}$ is the exchange current density for step 2; c_i is the concentration of intermediate species; $\bar{c}_i$ is the equilibrium concentration of intermediate species; β_1 is the anodic transfer coefficient for step 1; β_2 is the anodic transfer coefficient for step 2; and η is the anodic overpotential.

Adding Equations 11 and 12 and further simplifying provides the relation

$$i_a = \frac{2i_{0,1}\{\exp[\beta_1 F\eta/RT] - \exp[-(1-\beta_1)F\eta/RT]\}}{1 + i_{0,1}/i_{0,2}\exp[-(1+\beta_1-\beta_2)F\eta/RT]} \tag{13}$$

This equation and treatment is identical to that suggested by Vetter [17] for charge transfer processes which occur through a sequence of several charge transfer reactions. Wadsworth and Zhong [18] have used such a model to explain the anodic dissolution of Cu_2S when coupled with the cathodic reduction of ferric ion. Assuming that the first electron transfer (i.e. reaction 7) is the rate limiting step, then $i_{0,2} \gg i_{0,1}$ and for sufficiently large overpotential, Equation 13 becomes [17–19]:

$$i_a = 2i_{0,1}\exp\left(\frac{\beta_1 F\eta}{RT}\right) \tag{14}$$

A relationship similar to the Tafel equation, where the constants are somewhat different, can now be obtained from Equation 14.

$$\eta = a' + b' \log i_a \tag{15}$$

where

$$b' = \frac{2.303RT}{\beta_1 F} \tag{16}$$

Assuming a value of 0.5 for the transfer coefficients, β_1 and β_2, which seems quite reasonable [16, 17, 20], the Tafel slope can then be calculated from Equation 16 and compared with that estimated from the data in Fig. 4. Equation 16 would predict a Tafel slope of 0.118 V per decade. A two-electron transfer would indicate a Tafel slope of 0.059 V per decade. As can be seen from the data of Fig. 4 the observed Tafel slope is approximately 0.12 V per decade and thus in reasonable agreement with the proposed stepwise or sequential electron transfer reactions.

3.3. *Kinetic modelling of sulphate layer growth*

The abrupt levelling off of the current observed in Fig. 4 based on the results of cyclic voltammetry discussed earlier indicates the formation of Ag_2SO_4(s) due to saturation of the electrolyte near the Ag_2S surface. This is confirmed by the observation that no such abrupt change is observed for polarization curves in nitric acid where the solubility of Ag^+ is much higher as shown in Fig. 5. It is also obvious from Figs 4 and 5 that the product layer which forms must be porous, since the current remains constant and does not drastically decrease. The formation or growth of the Ag_2SO_4 product layer is analogous to oxide or passive layer formation on corroding surfaces and therefore the kinetics of film growth may be approached in a similar fashion. In the present case film growth was examined by holding Ag_2S electrodes at a constant anodic potential while monitoring the

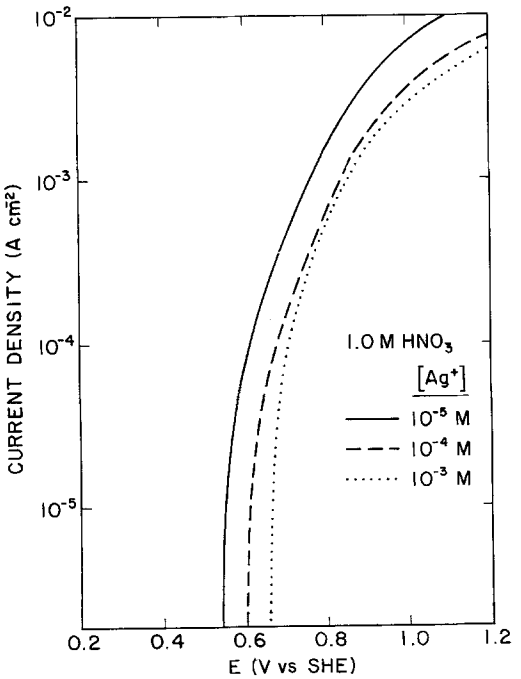

Fig. 5. Anodic polarization curves for a cast sample of Ag_2S in 1.0 M HNO_3 as a function of silver ion concentration. Sweep rate, 0.001 V s^{-1}.

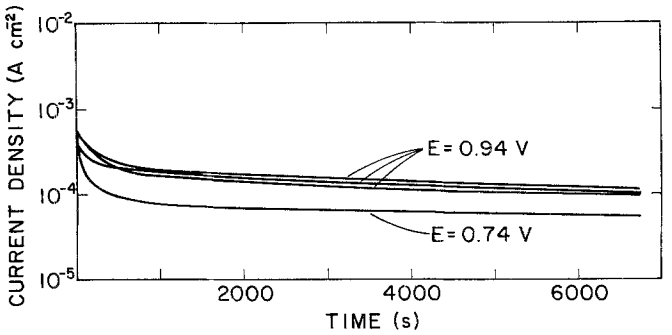

Fig. 6. Potentiostatic curves for a cast Ag_2S sample in 1.0 M H_2SO_4 at two applied potentials.

current as shown in Fig. 6. The potentiostatic curves have similar forms, reaching a rather constant current level soon after anodic treatment begins.

The film formation suggested by the data in Fig. 6 was examined through rate models and found to correlate quite well with a paralinear kinetic model. A schematic diagram of paralinear film growth is shown in Fig. 7a. Reactions exhibiting paralinear growth initially follow parabolic kinetics due to the growth of a thickening diffusion barrier or film which is produced at interface I. Over time, the adherence to parabolic kinetics is replaced by linear kinetics, which occur when the film achieves a steady state thickness, δ, and is removed at interface II at the same rate at which it is formed. The paralinear law is expressed by [21, 22]:

$$\frac{dQ}{dt} = \frac{k_p}{(Q - k_l t)} \tag{17}$$

The form of the equation is identical to that for parabolic film growth except for the second term in the denominator which accounts for the eventual shift to linear kinetics. The total charge passed, Q, has been assumed to be a reasonable estimate or replacement for the film thickness. Upon integration and rearrangement Equation 17 becomes

$$Q = k_l t + \frac{k_p}{k_l} - \frac{k_p}{k_l} \exp\left(\frac{-Qk_l}{k_p}\right) \tag{18}$$

The rate constants k_l and k_p can be evaluated from the slope and intercept of the linear portion of the plot as shown schematically in Fig. 7b. In this way the model may be tested by plotting an experimentally obtained Q versus time curve and comparing the results with an ideally paralinear curve. The charge passed was calculated from the potentiostatic curves in Fig. 6 by integration and the resulting Q versus time curves are displayed in Fig. 8. After approximately 4000 s, the curves show a change to linear kinetics. From the linear portion, the values of k_l and k_p have been estimated from the experimental data and are shown in Table 2. The constants thus obtained are used in Equation 18 to provide an ideally paralinear model which is compared with experimental data in

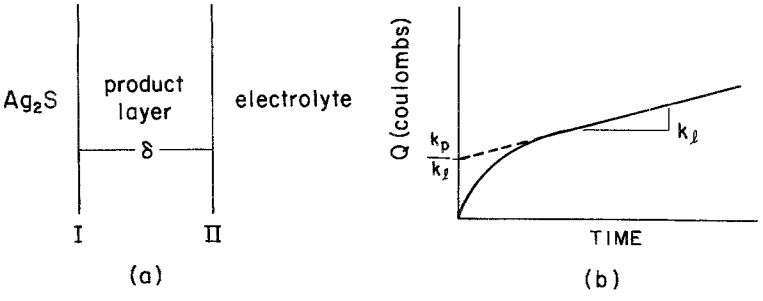

Fig. 7. (a) Schematic diagram of paralinear film growth. (b) Sketch of the paralinear model described by Equation 18. Rate constants can be obtained from the slope and intercept of the linear portion.

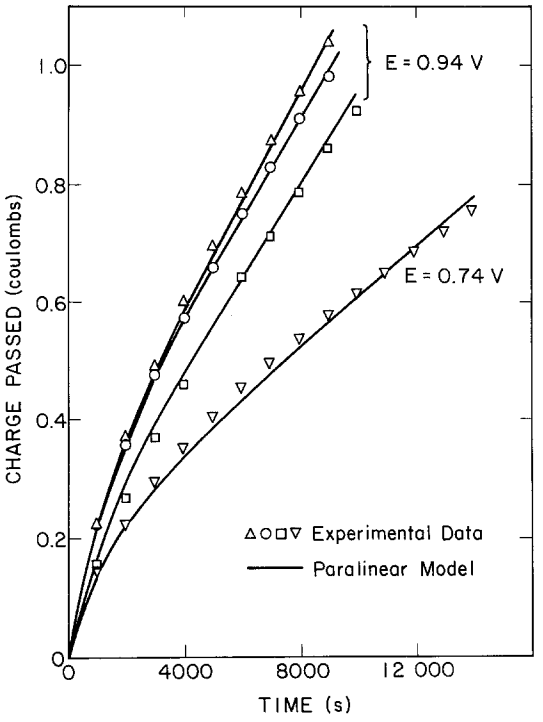

Fig. 8. A plot of charge passed versus time for the data given in Fig. 6.

Fig. 8. Agreement between the experimentally determined Q versus time curve and that calculated for an ideally paralinear curve is quite good. Other kinetic models were tested; however, none provided a better fit with experimental data. The values of k_l and k_p were fairly reproducible throughout trials.

The transition to linear kinetics may generally be attributed to either a rate-limiting surface reaction occurring at the metal–film or film–fluid interface, or the formation of a porous scale or a volatile or soluble product [23]. Considering the recognized formation of Ag_2SO_4 throughout the anodic treatment, the latter seems more likely. Therefore, the initial parabolic rate dependence of Ag_2S oxidation may be attributed to the accumulation of elemental sulphur and Ag_2SO_4 on the electrode surface, and the subsequent shift to linear kinetics suggests that this porous layer approaches a rate of dissolution equal to that of its formation. A similar model has been applied to the kinetics of anodic film formation on chalcopyrite electrodes in ammoniacal electrolytes [24].

3.4. *Diffusion control at higher overpotentials: rotating disc experiments*

At higher overpotentials the formation of a sulphate layer suggests that the dissolution of Ag_2S may

Table 2. Calculation of the paralinear constants from the experimental data given in Fig. 8.

Electrolyte	*Applied potential (V)*	k_l $(\times 10^{-5})$	$\frac{k_p}{k_l}$
1 M H_2SO_4	0.94	8.7	0.259
0.001 M H_2SO_4 + 0.999 M Na_2SO_4	0.94	8.4	0.244
1 M H_2SO_4	0.94	7.7	0.18
1 M H_2SO_4	0.74	4.1	0.211

be governed by the diffusion of Ag^+ through the boundary layer of the electrode. In order to examine this overpotential region, the rotating disc electrode (RDE) was employed. While the treatment of the hydrodynamic and convective–diffusion equations for the RDE are not shown here, the solutions are detailed elsewhere [17]. The common form of the solution is the Levich equation which, applied to Ag_2S dissolution, yields the limiting current as follows.

$$i = 0.620nFAD^{\frac{2}{3}}\omega^{\frac{1}{2}}\mu^{-\frac{1}{6}}(c_0^* - c_0) \tag{19}$$

where n is the equivalents per mole of Ag^+ produced = 1; D is the diffusivity; A is the electrode surface area; ω is the rotation speed, μ is the kinematic viscosity of the fluid; c_0^* is the concentration of species at the electrode surface; and c_0 is the concentration of species in the bulk solution.

Since this equation applies to the mass transfer-limited condition, it may be tested to determine the likelihood of a diffusion-limited mechanism for Ag_2S oxidation at higher overpotentials. By testing the fit between the equation and values obtained from experimental plots, the occurrence of a mass transfer-limited mechanism may be verified. More specifically, with the known values of n, F, A, μ, c_0^* and c_0 and with experimentally determined values of i and ω, the value for D of Ag^+ through the boundary layer may be calculated and compared with values from the literature.

The values of i and ω may be obtained from polarization curves such as those shown in Fig. 9. This plot shows a series of anodic polarization curves for pellet samples of Ag_2S with varying rotation speeds in 1 M H_2SO_4. As can be seen in the figure there is only a weak dependence on stirring speed, but it was generally true that stirring speeds in excess of approximately 260 r.p.m. resulted in higher currents than that observed in the absence of stirring. The lack of a strong dependence on rotation speed may be due to the presence of the sulphur and silver sulphate products which form on the surface. In addition, silver sulphate present in the pores of the sulphur would be less susceptible to changes in stirring rate. Using the data of Fig. 9 to estimate the diffusion coefficient for silver ion, it is assumed that c_0^* is the surface concentration of Ag^+ at saturation in 1 M H_2SO_4 solutions (0.071×10^{-3} mol cm^{-3}) and that the bulk concentration of silver ion is zero. Neglecting the surface area of the graphite, the area of the Ag_2S was 0.28 cm^2. Using Equation 19 and the limiting (peak) current value of 2.69×10^{-3}, a diffusion coefficient for Ag^+ of 0.19×10^{-5} and 0.11×10^{-5} cm^2 s^{-1} is calculated for 500 and 1000 r.p.m., respectively. The peak current was used, since this is the best representation of the limiting current before significant precipitation of silver sulphate occurs which would tend to decrease the effective area. This value compares

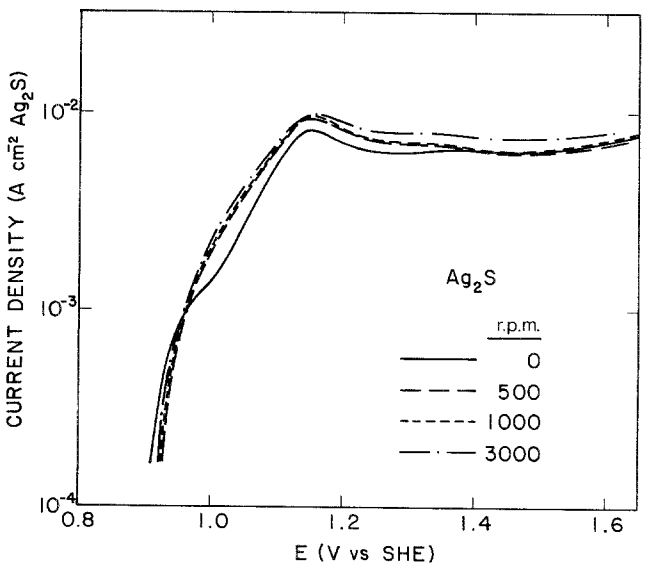

Fig. 9. Anodic polarization curves for rotating disc electrodes in 1.0 M H_2SO_4 as a function of the rotation speed. Sweep rate, 0.001 V s^{-1}.

reasonably well with the previously reported diffusion constant of $1.5 \times 10^{-5}\,cm^2\,s^{-1}$ for Ag^+ in similar solutions [20]. As a further comparison, using Fick's law and the reported value for the diffusion coefficient, a value of $1 \times 10^{-2}\,A\,cm^{-2}$ is calculated for the limiting diffusion current density, assuming a boundary layer thickness of 10^{-2} cm and $5 \times 10^{-2}\,A\,cm^{-2}$ for a thickness of 10^{-3} cm. These values compare well with the maximum currents observed in Figs 4 and 9.

4. Conclusions

The electrochemical behaviour of silver sulphate in sulphuric acid solutions has been delineated by means of cyclic voltammetry, potentiodynamic anodic polarization and constant potential experiments. The initial dissolution process is attributed to reaction 1. Based on a model developed from the Butler–Volmer relationship, this charge transfer reaction is suggested to occur through two sequential, single electron transfer steps, since the experimentally observed Tafel slopes are in reasonable agreement with that predicted from the model. The two sequential steps involve a short-lived intermediate sulphur species such as AgS or S^-. The model and the suggested intermediates are quite similar to those suggested by other investigators in similar dissolution mechanisms for metallic sulphides [5, 16–18].

When the current or dissolution rate increases, the electrolyte near the silver sulphide surface becomes saturated with dissolved Ag^+, and Ag_2SO_4(s) precipitates forming a porous product layer along with the elemental sulphur also produced from reaction 1. The rate of formation and growth of the product layer has been quantified in terms of a paralinear model for film growth which is initially parabolic and eventually changes to linear kinetics. The linear portion indicates that the film has achieved a relatively constant thickness and that the rate of film formation is equal to the rate of film dissolution. The rate of film dissolution should be a diffusion-limited process under these conditions, and this is supported by the reasonable agreement between the diffusion coefficient for Ag^+ calculated from rotating disc experiments and those reported in the literature. The results of cyclic voltammetry are consistent with the above conclusions and also indicate the reduction of dissolved Ag^+, when it is present, as well as the direct reduction of Ag_2S to metallic silver during the cathodic portion of the cycle.

These results show that dissolved Ag^+ will be present near an Ag_2S surface undergoing oxidation whether the rate of oxidation is low (i.e. low overvoltage) or high (i.e. high overvoltage). This could be significant if the dissolved Ag^+ is required for any catalytic reactions as has been suggested in the case of $CuFeS_2$ [1–3, 25]. Obviously a large portion of the silver may be tied up in the Ag_2SO_4 form, but the local concentration of Ag^+ near such precipitates would be reasonably high.

Acknowledgements

The authors gratefully acknowledge the support provided by the National Science Foundation primarily under Grant No. CPE-8108296, but also by equipment grants DMR-8001662 and DMR-8005380.

References

[1] G. J. Snell and M. C. Sze, *Eng. Mining J.* **178** (1977) 100.
[2] F. E. Pawlek, in '*Extractive Metallurgy of Copper*' (edited by J. C. Yannopoulos and J. C. Agarwal) AIME, New York (1976) p. 690.
[3] J. D. Miller and H. Q. Portillo, *Dev. Miner. Process.* **2** (1981) 851.
[4] G. W. Warren, B. Drouven and D. W. Price, *Metall. Trans. B* **15B** (1984) 235.
[5] R. L. Paul, M. J. Nicol, J. W. Diggle and A. P. Saunders, *Electrochim. Acta* **23** (1978) 625.
[6] B. Dandapani and E. Ghali, *Trans. Instn. Min. Metall.* **91** (1982) 38.
[7] R. A. Narasgoudar, J. W. Johnson, and T. J. O'Keefe, *Hydrometallurgy* **9** (1982) 37.
[8] T. Biegler and D. A. Swift, *J. Appl. Electrochem.* **9** (1979) 545.

[9] B. Dandapani and E. Ghali, *J. Electrochem. Soc.* **129** (1982) 271.
[10] M. H. Lietzke and R. W. Stoughton, *J. Phys. Chem.* **65** (1961) 2247.
[11] *Idem*, *J. Amer. Chem. Soc.* **78** (1956) 3023.
[12] J. Gulens and D. W. Shoesmith, *J. Electrochem. Soc.* **128** (1981) 811.
[13] V. I. Birss and G. A. Wright, *Electrochim. Acta* **27** (1982) 1.
[14] J. O'M. Bockris and G. A. Razumney, '*Fundamental Aspects of Electrocrystallization*', Plenum Press, New York (1967) p. 36.
[15] J. B. Hiskey, *Inst. Min. Metall.* **88C** (1979) 145.
[16] M. J. Nicol, R. L. Paul and J. W. Diggle, *Electrochim. Acta* **23** (1978) 635.
[17] K. J. Vetter, '*Electrochemical Kinetics*', Academic Press, New York (1967) pp. 149–53.
[18] M. E. Wadsworth and T. K. Zhong, in '*Hydrometallurgical Process Fundamentals*' (edited by R. G. Bautista), Plenum Press, New York (1984).
[19] J. O'M. Bockris and A. K. N. Reddy, '*Modern Electrochemistry*', Plenum Publishing Co., New York (1973) pp. 1291–5.
[20] A. R. Despic and J. O'M. Bockris, *J. Chem. Phys.* **32** (1960) 389.
[21] P. Kofstad, '*High Temperature Oxidation of Metals*', John Wiley, New York (1966) pp. 1–19.
[22] J. H. Ahn, PhD dissertation, Department of Metallurgical Engineering, University of Utah, Salt Lake City, Utah (1985).
[23] E. W. Haycock, *J. Electrochem. Soc.* **106** (1959) 771.
[24] G. W. Warren and M. E. Wadsworth, *Metall. Trans. B* **15B** (1984) 289.
[25] D. W. Price and G. W. Warren, *Hydrometallurgy* **15** (1986) 303.